Spin-Dependent Phase Diagram of the $\nu_T = 1$ Bilayer Electron System

P. Giudici,[1] K. Muraki,[1] N. Kumada,[1] Y. Hirayama,[1,2,*] and T. Fujisawa[1]

[1]NTT Basic Research Laboratories, NTT Corporation, 3-1 Morinosato-Wakamiya, Atsugi 243-0198, Japan

[2]SORST-JST, 4-1-8 Honmachi, Kawaguchi 331-0012, Japan

(Received 23 March 2007; published 12 March 2008)

We show that the spin degree of freedom plays a decisive role in the phase diagram of the $\nu_T = 1$ bilayer electron system using an in-plane field $B_\parallel$ in the regime of negligible tunneling. We observe that the phase boundary separating the quantum Hall and compressible states at $d/\ell_B = 1.90$ for $B_\parallel = 0$ (d: interlayer distance, ℓ_B: magnetic length) steadily shifts with $B_\parallel$ before saturating at $d/\ell_B = 2.33$ when the compressible state becomes fully polarized. Using a simple model for the energies of the competing phases, we can quantitatively describe our results. A new phase diagram as a function of d/ℓ_B and the Zeeman energy is established and its implications as to the nature of the phase transition are discussed.

DOI: 10.1103/PhysRevLett.100.106803 PACS numbers: 73.43.Nq, 71.10.Pm, 73.21.−b

Two-dimensional electron systems under a strong perpendicular magnetic field have been continually revealing a wide variety of new phenomena that arise from electron-electron interactions. Multilayered systems have further opened a new realm for many-body effects as a consequence of the layer degree of freedom. In particular, a bilayer system at total filling factor $\nu_T = 1$ involves tremendously rich physics [1]. An experimental phase diagram established by Murphy *et al.* [2] shows that the system undergoes a phase transition between quantum Hall (QH) and compressible states as a function of two parameters: the tunneling gap Δ_{SAS} and d/ℓ_B, the latter representing the ratio between the intra- and interlayer Coulomb energies, where d and ℓ_B are the interlayer distance and the magnetic length, respectively. Of particular interest is the limit of $\Delta_{SAS} \to 0$, where a purely many-body QH state with spontaneous interlayer phase coherence emerges below a critical value of d/ℓ_B. This new state can be described as an excitonic condensate [3–5] or a pseudospin ferromagnet [1,6], with the pseudospin encoding the layer degree of freedom. Experiments have established that for $\Delta_{SAS} \approx 0$ the QH-compressible phase transition takes place at $d/l_B \sim 2$ [2,7], though its exact nature remains an open issue [7–10].

An in-plane field $B_\parallel$ has often been used as an additional tool to modify the properties of bilayer systems [2,6,11]. Its primary effect is to suppress the interlayer tunneling and reduce Δ_{SAS} [12]. The tunneling suppression can lead to the destruction of the QH state when the system is close to the phase boundary with the compressible state [11]. Additionally, an anomalous response of the $\nu_T = 1$ QH state to $B_\parallel$, where the quasiparticle gap first drops abruptly and then stays at a finite value, is observed [2] and interpreted in terms of a commensurate-incommensurate transition [13]. In these studies, only the effects of $B_\parallel$ on the orbital part of the electron wave function have been considered, under the assumption that the spin degree of freedom is frozen by the magnetic field. Although recent experiments indicate that this assumption no longer holds in the relevant magnetic field region [14,15], it is still generally understood that spin plays only a minor role in the property of the $\nu_T = 1$ system.

In this Letter, we demonstrate that spin plays a decisive role in the phase diagram of the $\nu_T = 1$ system in the regime of negligible tunneling. In marked contrast to the previous results for finite Δ_{SAS}, we find that the QH state is strengthened by applying $B_\parallel$ and can be even restored at high densities where the QH effect is absent for $B_\parallel = 0$. Upon increasing $B_\parallel = B_{TOT} \sin\theta$ by tilting the sample by an angle θ away from the external field B_{TOT}, the phase boundary shifts toward higher values from $d/\ell_B = 1.90$ at $\theta = 0°$ and eventually saturates at $d/\ell_B = 2.33$ for $\theta \gtrsim 60°$ ($B_{TOT} \gtrsim 8$ T). A simple model considering the Coulomb and Zeeman energies of the two phases provides an excellent fit to the observed $B_\parallel$ dependence, demonstrating that the increased Zeeman energy makes the partially polarized compressible state energetically unfavorable at high B_{TOT}. The saturation at large $B_\parallel$ indicates the full polarization of the compressible state. A new phase diagram as a function of d/ℓ_B and the Zeeman energy is established and its implications as to the nature of the phase transition are discussed.

The sample, a modulation-doped double quantum well grown by molecular-beam epitaxy, consists of two 18-nm-wide GaAs wells separated by a 10-nm-thick barrier consisting of alternating layers of AlAs (2.1 nm) and GaAs (0.56 nm). Δ_{SAS} for this structure is calculated to be 150 μK. A Hall bar mesa was made by conventional photolithography. In the as-grown situation, only the upper layer is populated with an electron density of 5×10^{10} cm^{-2} and a low-temperature mobility of 1×10^6 cm^2/V s. By applying front- and back-gate biases, the electron densities in the upper and lower layers can be controlled independently. To confirm that the tunneling is negligible, additional gates (hereafter isolation gates) are included so that the upper layer is disconnected from the contacts except the one for the ground. We work at the balance condition, with equal densities in the two layers, and tune d/ℓ_B through the total electron density n_T. We take for the interlayer distance d the well center-to-center distance of 28 nm, which has an uncertainty of 5%. Unless otherwise specified, measurements were performed without applying isolation gates and at a temperature of about 100 mK with the sample placed in the mixing chamber of a dilution refrigerator.

Figure 1 shows the longitudinal (R_{xx}) and Hall (R_{xy}) resistances taken at $\theta = 0°$ as a function of the magnetic field for a total density $n_T = 6.8 \times 10^{10}$ cm^{-2}. Solid lines correspond to the standard configuration, where both layers are connected in parallel. At this density, the $\nu_T = 1$ QH state is well developed because the parameter $d/\ell_B = 1.83$ is below the critical value in our sample, $d/\ell_B = 1.90$. When the upper layer is disconnected using the isolation gates (dashed lines), at low fields the Hall resistivity is doubled with plateaus at twice as high values, reflecting the electron density of a single layer. This observation confirms that the tunneling is negligible in this sample. At $\nu_T = 1$, R_{xy} suddenly returns to the bilayer value of h/e^2, indicating that the $\nu_T = 1$ QH state bears spontaneous interlayer phase coherence, as reported in Refs. [3–5,7].

Figure 2 displays R_{xx} and R_{xy} against perpendicular field $B_\perp$ taken at a higher density of $n_T = 8.5 \times 10^{10}$ cm^{-2}, which corresponds to $d/\ell_B = 2.05$. As expected for this high value of d/ℓ_B, the $\nu_T = 1$ QH state is not present at $\theta = 0°$ (dashed lines). The traces change drastically when the sample is tilted at $\theta = 52°$ (solid lines): the $\nu_T = 1$ QH state is restored and a clear minimum in R_{xx} as well as a plateau in R_{xy} at $\nu_T = 1$ become apparent. We emphasize that the electron density is kept constant and the only effect exerted on the system by tilting is to introduce an in-plane field component. The inset of Fig. 2 illustrates the evolution of the R_{xx} minimum with tilt from $\theta = 6°$ to $58°$. From the continuous evolution of the R_{xx} minimum, it is clear that the QH state is stabilized by the in-plane field. The observed behavior is totally opposite to the previous reports for samples with large Δ_{SAS}, where the $\nu_T = 1$ QH state is known to be weakened by an in-plane field. Our calculations of the wave function under a tilted magnetic field show that the change in the effective interlayer distance is less than 0.1%. Considering this result and the negligible tunneling in our sample, we can rule out the effects of $B_\parallel$ on the orbital part of the wave function.

To evaluate the effect of $B_\parallel$ on the stability of the $\nu_T = 1$ QH state, we examined for different θ the density at which the QH state collapses into the compressible state. Figure 3 shows the evolution with density of R_{xx} around $\nu_T = 1$, plotted against $B_\perp$. Top and bottom panels show results for $\theta = 0°$ and $52°$, respectively. At $\theta = 0°$, the $\nu_T = 1$ QH state survives up to $B_\perp \simeq 3$ T, corresponding to $d/\ell_B = 1.9$, a value consistent with previous reports [2,7,14]. At $\theta = 52°$, the QH state is still well preserved at $B_\perp = 3$ T and the transition occurs at a much higher field of $B_\perp \simeq 4$ T, which corresponds to an unexpectedly high value of $d/\ell_B = 2.2$. The same is confirmed by the activation gap measurements as shown in the inset of Fig. 3(a), demonstrating that the gap, which vanishes at $B_\perp = 3.10 \pm 0.05$ T for $\theta = 0°$, remains finite up to 4.60 ± 0.05 T when the sample is tilted at an angle of 61°.

We have determined the critical density $n_T = eB_\perp/h$ at which the R_{xx} minimum disappears for ten different angles from $\theta = 0°$ to $62°$; the results are shown in Fig. 4(a) as a function of B_{TOT}. Solid symbols represent the maximal density at which the QH state is still observed and open symbols the density at which the QH state has disappeared.

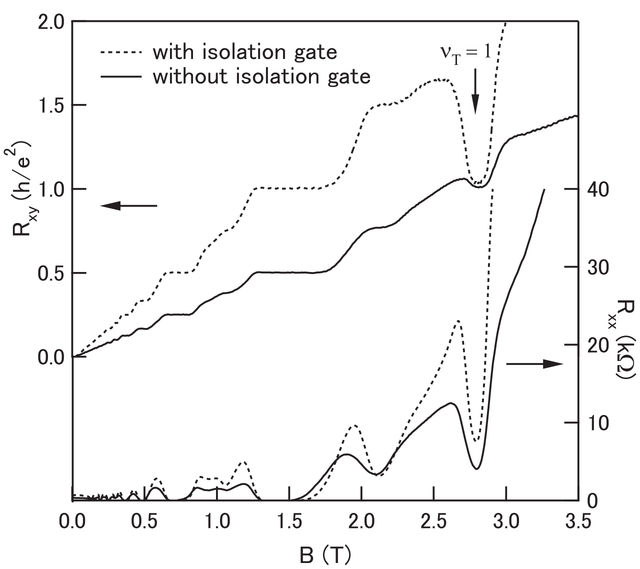

FIG. 1. Longitudinal and Hall resistances as a function of magnetic field at a total density of $n_T = 6.8 \times 10^{10}$ cm^{-2}, which corresponds to $d/\ell_B = 1.83$. Solid (dashed) lines are obtained without (with) an isolation gate bias.

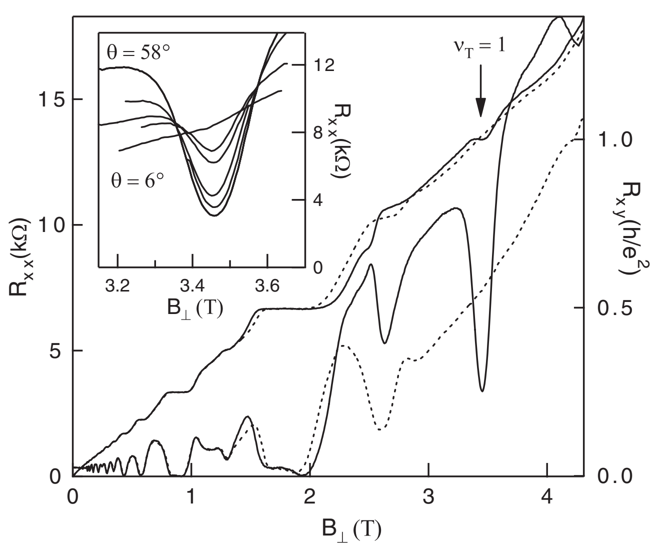

FIG. 2. R_{xx} as a function of the perpendicular magnetic field, for two angles, $\theta = 0°$ (dashed lines) and $52°$ (solid lines), at the fixed density of $n_T = 8.5 \times 10^{10}$ cm^{-2}, corresponding to $d/\ell_B = 2.05$. Inset: evolution of the minimum at $\nu_T = 1$, upon tilting the sample by $\theta = 6°$, $30°$, $44°$, $49°$, $52°$, and $58°$.

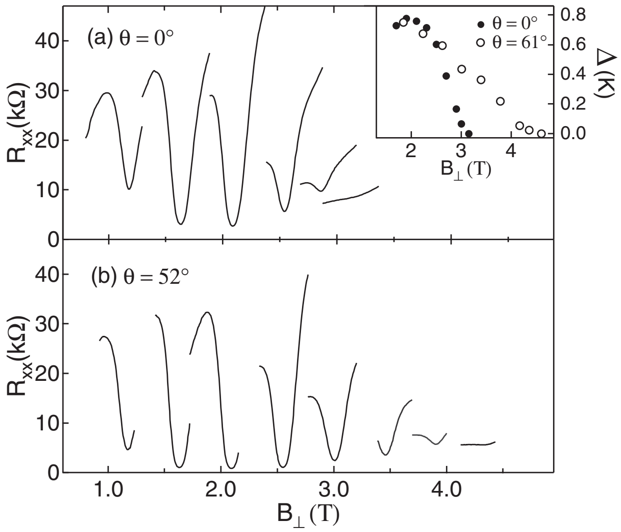

FIG. 3. R_{xx} around $\nu_T = 1$ at different densities as a function of the perpendicular magnetic field. Two sets are plotted for (a) $\theta = 0°$ and (b) $\theta = 52°$. Inset: energy gap Δ for $\theta = 0°$ and $61°$ at different densities, obtained from the temperature dependence of $R_{xx} \propto \exp(-\Delta/2T)$, measured between 40 and 500 mK.

Figure 4(a) shows the intriguing finding that an increase in B_{TOT} moves the transition to higher densities until it saturates at a value of $n_T = 11 \times 10^{10}$ cm^{-2} for $B_{\mathrm{TOT}} \geq 8$ T ($\theta \geq 58°$). We speculate that the observed behavior is due to the Zeeman energy, an indication that the competing states at the phase boundary have different degrees of spin polarization. This assertion is in line with the recent report of Spielman *et al.* [14], who have shown that the spin polarization of the QH state is higher than that of the compressible state.

To confirm this idea, we develop a simple model considering the Coulomb and Zeeman energies of the QH and compressible states. At zero temperature, the phase transition occurs when the energies of the two states become equal, a condition that can be modeled as

$$\alpha \frac{e^2}{4\pi\epsilon\ell_B} + \beta \frac{e^2}{4\pi\epsilon d} - \frac{E_Z}{2} = (1 + p^2)\frac{E_F}{4} - p\frac{E_Z}{2}, \quad (1)$$

where the left- and right-hand sides correspond essentially to the QH and compressible states, respectively. The terms proportional to ℓ_B^{-1} and d^{-1} represent the intra- and interlayer Coulomb energies, respectively, where α and β are unknown prefactors and ϵ the dielectric constant of GaAs. $E_Z/2$ is the Zeeman energy of a fully polarized system, as commonly accepted for the $\nu_T = 1$ QH state ($E_Z = g\mu_B B_{\mathrm{TOT}}$, with $g = 0.44$ for GaAs). We further assume that the compressible state consists of two nearly independent layers at $\nu = 1/2$, which in the composite-fermion (CF) framework can be effectively mapped onto a Fermi liquid at zero magnetic field [16]. Interlayer interactions in the compressible state, if present, can be absorbed in the d^{-1} term on the left-hand side, which then represents the difference in the interlayer energies between the two phases. Additionally, the single-layer $\nu = 1/2$ state is known to be only partially polarized at low fields [17]. These considerations allow us to express the intralayer Coulomb energy of the compressible state in terms of the kinetic energy of a partially polarized paramagnet with a Fermi surface for each spin component. This is given by the term $\frac{1}{4}(1 + p^2)E_F$, where $p = (n^{\uparrow} - n^{\downarrow})/n = E_Z/E_F$ is the spin polarization and $E_F = 2\pi\hbar^2 n/m_{\mathrm{CF}}$ the Fermi energy of a fully polarized CF system, with $n = n_T/2$ the density per layer and m_{CF} the CF effective mass. Taking $E_C = e^2/4\pi\epsilon\ell_B$ as a unit of energy, Eq. (1) can be written in the following dimensionless form:

$$\alpha + \beta\frac{\ell_B}{d} = -\frac{1}{4C}(\eta - C)^2 + \frac{C}{2}, \quad (2)$$

where $\eta = E_Z/E_C$ and $C = E_F/E_C$ are the normalized Zeeman and Fermi energies, respectively. Using the relation $m_{\mathrm{CF}} \propto \sqrt{B_\perp}$ [18], C is found to be a constant, and the model allows a simple analytic expression of ℓ_B/d as a quadratic function of η for $\eta < C$. When the system becomes fully polarized at $\eta \geq C$ ($p = E_Z/E_F = 1$),

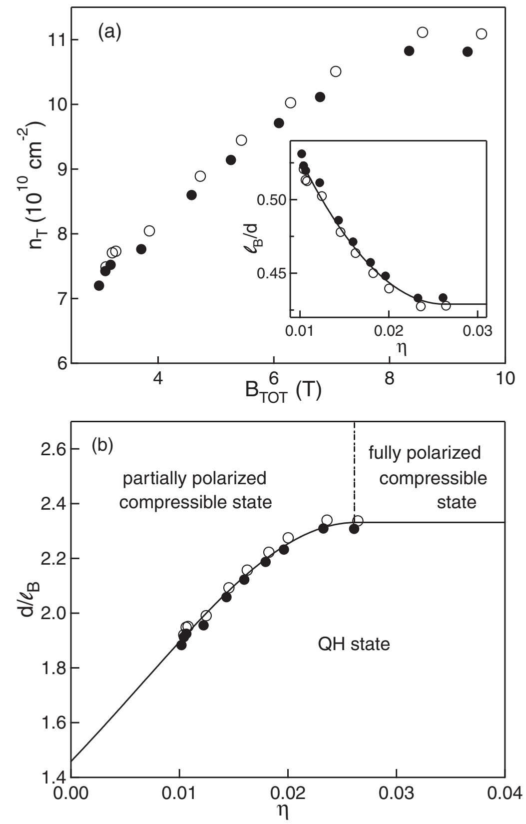

FIG. 4. Transition point between the compressible and QH states plotted in three different ways. (a) Critical density as a function of total magnetic field. Inset) Critical ℓ_B/d as a function of the normalized Zeeman energy η. (b) Phase diagram in the d/ℓ_B-η space. Solid (open) circles correspond to the QH (compressible) state and lines to the fit result. The dashed line indicates $\eta = C$.

Eq. (1) comes to be independent of the Zeeman energy and ℓ_B/d reduces to a constant. In the inset of Fig. 4(a), we replot the data as ℓ_B/d against η, and we fit them using the proposed function, with α, β, and C as fitting parameters. The fitting with the model is excellent, yielding $\alpha = 0.024 \pm 0.001$, $\beta = -0.025 \pm 0.002$, and $C = 0.026 \pm 0.001$. The negative sign of β is inherent to the stability of the QH state at lower fields. From $C = 0.026 \pm 0.001$, we determine the CF effective mass $m_{CF} = (0.52 \pm 0.02)\sqrt{B_\perp} m_0$ (m_0 is the electron mass in vacuum). The prefactor of 0.52 is in reasonably good agreement with the theoretical value of 0.6 [18] and the experimental value of 0.74 [17] for a single layer at $\nu = 1/2$, if we consider the different sample structures.

Based on our experimental data and analysis, we are able to construct a new phase diagram in the d/ℓ_B-η plane at $\Delta_{SAS} = 0$ [Fig. 4(b)], complementary to the standard phase diagram in the d/ℓ_B-Δ_{SAS} plane [2]. The new phase diagram reveals that the intrinsic transition point for the ideal spinless system is $d/\ell_B = 2.33$, 23% higher than $d/\ell_B = 1.90$ at $\theta = 0°$. This has important implications on the nature of the phase transition. Using the parameters obtained from the fitting, the spin polarization of the compressible state at the transition is estimated to be only $p = 0.4$ for $\theta = 0°$, in contrast to $p = 1$ for the QH state. By a general argument, a level crossing between states with different spin configurations implies a first-order transition. This assertion is consistent with the strong enhancement of longitudinal drag at the transition [7] and its explanation in terms of the coexistence of compressible and incompressible domains [9]. We also note that the collapse of the $\nu_T = 1$ QH state is often explained as being due to a charge-density instability associated with a softening at a finite wave vector of a collective mode [19,20]. However, if the mode does not involve spin as usually accepted [6], it is independent of the Zeeman energy and therefore should be irrelevant to the transition to the partially polarized compressible state. This in turn suggests that the experimentally observed transition is governed by a different mechanism. On the other hand, in the limit of high magnetic fields, the transition from the QH state to the fully polarized compressible state does not necessarily have the same character as the one to the partially polarized compressible state. When $p = 1$, the Zeeman terms in Eq. (1) cancel each other and the phase boundary is determined solely by the Coulomb terms, making the above argument irrelevant. In fact, theories predict various scenarios for a spinless system [8,10].

The diagram in Fig. 4(b) additionally presents many intriguing suggestions. First, the standard d/ℓ_B-Δ_{SAS} phase diagram would have to be modified to incorporate the spin effects. Second, in the limit of $\eta \to 0$, where one expects a new QH state with both spin and pseudospin broken symmetry, the phase boundary should be at $d/\ell_B \sim 1.5$. Experimentally, this limit can be achieved by applying a hydrostatic pressure [21]. Third, the striking role of spin on the phase diagram suggests that hole systems, which have a larger g factor and hence a larger Zeeman splitting [22], may behave differently from electron systems; this may explain some of the differences in the behavior of hole systems [4].

In conclusion, we have demonstrated that the QH-compressible phase boundary in the $\nu_T = 1$ system is strongly dependent on the spin degree of freedom, being the nature of the phase transition contingent on the spin polarization of the compressible state.

---

*Present address: Department of Physics, Tohoku University, Sendai 980-8578, Japan.

[1] S. M. Girvin and A. H. MacDonald, *Perspectives in Quantum Hall Effects*, edited by A. Pinczuk and S. Das Sarma (Wiley, New York, 1997).

[2] S. Q. Murphy *et al.*, Phys. Rev. Lett. **72**, 728 (1994).

[3] M. Kellogg, J. P. Eisenstein, L. N. Pfeiffer, and K. W. West, Phys. Rev. Lett. **93**, 036801 (2004).

[4] E. Tutuc, M. Shayegan, and D. A. Huse, Phys. Rev. Lett. **93**, 036802 (2004).

[5] R. D. Wiersma *et al.*, Phys. Rev. Lett. **93**, 266805 (2004).

[6] I. B. Spielman, J. P. Eisenstein, L. N. Pfeiffer, and K. W. West, Phys. Rev. Lett. **87**, 036803 (2001).

[7] M. Kellogg, J. P. Eisenstein, L. N. Pfeiffer, and K. W. West, Phys. Rev. Lett. **90**, 246801 (2003).

[8] J. Schliemann, S. M. Girvin, and A. H. MacDonald, Phys. Rev. Lett. **86**, 1849 (2001).

[9] A. Stern and B. I. Halperin, Phys. Rev. Lett. **88**, 106801 (2002).

[10] S. H. Simon, E. H. Rezayi, and M. V. Milovanovic, Phys. Rev. Lett. **91**, 046803 (2003); D. N. Sheng, L. Balents, and Z. Wang, *ibid.***91**, 116802 (2003); N. Shibata and D. Yoshioka, J. Phys. Soc. Jpn. **75**, 043712 (2006).

[11] S. Luin *et al.*, Phys. Rev. Lett. **97**, 216802 (2006).

[12] J. Hu and A. H. MacDonald, Phys. Rev. B **46**, 12 554 (1992); G. S. Boebinger, H. W. Jiang, L. N. Pfeiffer, and K. W. West, Phys. Rev. Lett. **64**, 1793 (1990).

[13] Kun Yang *et al.*, Phys. Rev. Lett. **72**, 732 (1994).

[14] I. B. Spielman *et al.*, Phys. Rev. Lett. **94**, 076803 (2005).

[15] N. Kumada, K. Muraki, K. Hashimoto, and Y. Hirayama, Phys. Rev. Lett. **94**, 096802 (2005).

[16] B. I. Halperin, P. A. Lee, and N. Read, Phys. Rev. B **47**, 7312 (1993).

[17] I. V. Kukushkin, K. v. Klitzing, and K. Eberl, Phys. Rev. Lett. **82**, 3665 (1999).

[18] K. Park and J. K. Jain, Phys. Rev. Lett. **80**, 4237 (1998).

[19] H. A. Fertig, Phys. Rev. B **40**, 1087 (1989).

[20] A. H. MacDonald, P. M. Platzman, and G. S. Boebinger, Phys. Rev. Lett. **65**, 775 (1990).

[21] D. R. Leadley *et al.*, Phys. Rev. Lett. **79**, 4246 (1997).

[22] K. Muraki and Y. Hirayama, Phys. Rev. B **59**, R2502 (1999).